International Journal of Rock Mechanics and Mining Sciences 115 (2019) 137–144

Contents lists available at ScienceDirect

International Journal of Rock Mechanics and Mining Sciences

journal homepage: www.elsevier.com/locate/ijrmms

Frequency analysis of multi-sources acoustic emission from high-velocity waterjet rock drilling and its indicator to drilling efficiency

Mao Sheng[a,b,*], Shouceng Tian[a,b], Bo Zhang[c], Hongkui Ge[a,d]

[a] State Key Laboratory of Petroleum Resources and Prospecting, (China University of Petroleum-Beijing), Beijing 102249, PR China
[b] College of Petroleum Engineering, China University of Petroleum-Beijing, Beijing 102249, PR China
[c] Department of Geological Sciences, University of Alabama, USA
[d] College of Petroleum Engineering, China University of Petroleum-Beijing at Karamay, Karamay 834000, PR China

ARTICLE INFO

Keywords:
Acoustic emission
Waterjet
Rock failure

ABSTRACT

Acoustic emission has been recognized as a potentially advanced technique to monitor the efficiency of high-velocity waterjet rock drilling. Identification of AE multi-sources signals becomes fundamental to correlate AE singles and rock drilling efficiency. This paper presents a controlled experimental scheme and frequency analysis to identify different signal sources from waterjet impact and rock failure, respectively. Acoustic signals were decomposed into low, medium, and high-frequency signals by using the variational mode decomposition (VMD) approach. Results indicate that the waterjet impact generates a wideband acoustic signal. The frequency distribution of the high-frequency signals exhibited a strong diversity among four materials because of their different acoustic attenuation. Furthermore, the waterjet pressure did not change the frequency domain distribution of the material. An obvious reduction of the high-frequency signals was observed while waterjet rock drilling. Furthermore, the main frequency of high-frequency signals starts to be time-dependent that causes from the rock failure process. The high-frequency band presented a good correlation with the rate of penetration.

1. Introduction

Acoustic emission (AE) technique becomes an advanced technique to detect high strain failure process of metal and rock materials.[1,2] Waterjet rock drilling is a typical high-velocity impact process.[3] The principle of waterjet is generating a high water pressure and flow through a nozzle to form a high velocity and impact force jet, therefore the live detection of the velocity become essential on the success of waterjet technology. Up until now, sensing techniques are still scarce and require expensive online monitor for the waterjet rock drilling quality evaluation.[4] Our recent work suggested the feasibility of AE monitoring downhole failure process of the rock under waterjet impact.[5] Furthermore, AE signals of waterjet rock drilling come from waterjet impact and rock failure.[4] Thus, an inner understanding of the AE source mechanisms and identifying the AE sources from either waterjet impact or rock failure become essential for both fundamental and applied petroleum scientists and engineers.

Previous literatures studied the quality of waterjet precise machining by the correlation of AE energy and drilling performance. For instance, Mohan et al.[6] was the first to provide a framework for the online monitoring of depth of Abrasive Waterjet (AWJ) using acoustic emission. Kovacevic et al.[4] studied the material removal mechanisms by the stochastic modeling of AE signals and concluded the Root Mean Square (RMS) was a promising tool for monitoring the depth of AWJ drilling. Momber et al.[7,8] integrated AE technique and optical microscopy investigations to determine the erosion process of concrete material and confirmed that the AE signal is capable of identifying the failure mode very effectively. Furthermore, Momber and Kovacevic[9] quantified the energy dissipation in AWJ machining through linking the AE signals to a physical energy dissipation model. Hassan[10] proposed a model for the online depth of cut monitoring based on AE response and observed the linear correlation of RMS and cutting depth. Axinte and Kong[11] presented an integrated energy-based monitoring method to detect anomalous events occurring at both nozzle and workpiece. Rabani et al.[12] proposed an AE energy transfer rate that links the input jet energy, area of the abraded footprint, and jet feed velocity. Previous works provided the strong feasibility of AE on-line monitoring for sensing drilling process and underlying mechanisms. However, the AE source mechanisms and their identities have yet to be addressed, which would still be insufficient to identify the individual AE energy of fluid dynamics and rock failure.

In this paper, we designed - series of controlled experiments to

* Corresponding author at: College of Petroleum Engineering, China University of Petroleum-Beijing, 102249 Beijing, PR China.
E-mail address: shengmao@cup.edu.cn (M. Sheng).

https://doi.org/10.1016/j.ijrmms.2019.01.005
Received 21 December 2018; Accepted 19 January 2019
Available online 07 February 2019

measure the single-source signal purely from waterjet and the multi-source signals from the waterjet rock drilling process, respectively. An advanced signal analysis method, named as Variational Mode Decomposition, was used to decompose the AE signals into several Intrinsic Mode Functions (IMFs) that represent the individual source mechanism. Their corresponding source was interpreted by comparing the changes of dominant frequency before and after rock failure. Moreover, we correlated the drilling parameters and high-frequency signals of various sources. This work provides more insight into the AE source mechanisms.

2. Materials and methods

2.1. Experimental setup and scheme

A series of waterjet rock drilling tests were conducted on a KMT® three-axial waterjet cutting system. The system consists of a KMT streamline SL-V-50 high-pressure pump by providing a maximum pressure of 380 MPa, cutting head, metering system, and Computer Numerical Control (CNC). The accuracy of distance control reaches 0.1 mm. The PAC® digital AE system was used to record the continuous AE wave with a high sampling rate of 3 MHz and 40 dB pre-amplification. Because of drilling fluid circulation, the waterjet and rock target was required submerging in a water tank. One underwater AE sensor with an integral preamplifier (Model: PAC® R30I-UC with broadband of 200–400 kHz and the resonate frequency: 350 kHz) was used to satisfy the underwater environment. The AE sensor was mounted on the cylinder surface of the rock target and was one-third of length apart from the top surface in order to reduce the wave propagation path (Fig. 1). Our previous work confirms the broadband AE sensor is able to cover the frequency range generated by waterjet rock drilling.[5]

The recording signals of waterjet rock drilling process represent a synthetic signal containing information from not only rock failure behaviors but also the turbulent flow of high-velocity waterjet. The hypothesis is that one certain source corresponds to a specific main frequency. In order to identify the sources of AE signals, one experimental group was designed on rock materials to receive the synthetic signal; and the other control group was prepared to measure the AE signal purely generating from waterjet impact. The control group kept waterjet pressure below the yield stress of the target material to ensure no material failure. Thus, the AE signals from material failures can be eliminated. A low waterjet pressure (50–60 MPa) was used to satisfy the requirement of no material failure. The receiving signals were the acoustic wave induced by waterjet impact but not the acoustic emission because of no material failure. Besides, a high waterjet pressure (over 230 MPa) was used for rock drilling. The detailed waterjet parameters were listed in Table 1.

2.2. Materials and procedure

Three typical sedimentary rocks, the Longmaxi shale, and Junnggar tight sandstone, and Wumishan limestone were selected as our rock drilling targets (Fig. 2). Differences in rock strength, mineral structure, and failure behaviors between these rockThe shale samples for this study were collected from the outcrop of Lower Silurian Longmaxi unconventional shale gas formation in Sichuan Basin, China. The content of organic matter reaches to 2.5% weight. Furthermore, shale has ultralow permeability and porosity with the values of 9.88×10^{-3} mD and 2.87%, respectively. The sandstone samples were collected from the outcrop of Badaowan natural gas formation in Junggar Basin, China. The limestone samples were collected from the outcrop of Wumishan geothermal formation in Beijing, China. The mineralogical composition of the Longmaxi shale and Junnggar sandstone was shown in Fig. 3.

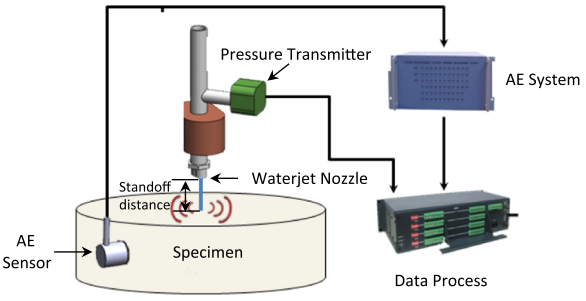

Fig. 1. Schematic of experimental setup building on a KMT waterjet cutting system and PAC digital AE system (a) and its photograph (b).

In order to exclude the AE signals from material failure, a high strength AISI 1045 steel was selected as a control group and the waterjet pressure was controlled below the yield stress of AISI 1045 steel to make sure the steel cannot fail under high-velocity waterjet impact. The rock mechanical properties were measured through standard ISRM recommended methods as listed in Table 2.

To ensure enough wave transmission time, the sample size was designed as 100 mm in both diameter and length. All samples were cored from the same outcrop block and the fine polish by 1600 mesh sandpaper ensured that the samples' top and bottom surface were parallel within 100 μm or less.

The experimental procedure can be summarized as (i) Sample and AE sensors were installed in which sample holder was designed to fix the sample and adjust the horizons of the top surface. A rubber band was used to fasten the AE sensors contact with the sample surface. (ii) The standoff distance of waterjet was adjusted into a constant value of 2 mm. The standoff distance is the gap distance from the nozzle outlet to the sample top surface (as illustrated in Fig. 2). (iii) Continuously waterjet rock drilling was applied on the target for 1 min. (iv) AE signals were continuously recorded for the first twenty seconds of every minute. (v) The drilling time was changed into 3, 4, 5, 6, 7, 8 min. At last, eight AE signal datasets and drilling holes were obtained. vi) Data processing: Only 0.02 s AE data were analyzed one time to satisfy the computer capability to satisfy the PC data processing capacity.

Two experimental schemes for the control group and experimental group were summarized in Table 3. For the control group, the waterjet pressure was set 50–60 MPa below the yield strength of the material to avoid the material failure under high-velocity waterjet impact. The waterjet pressure was enhanced into 230 MPa for waterjet rock drilling. Particularly, the AISI 1045 steel was still strong enough to resist the waterjet regardless of the high and low waterjet pressure.

2.3. Signal processing methodology

The frequency spectrum is an important indicator to identify the frequency variation of AE signals. The signal decomposition becomes a required technique to provide high-resolution signals in different frequency bands. The Variational Mode Decomposition (VMD) method is a newly developed methodology that promised higher spectral and spatial resolution compared with the short-time Fourier transform or wavelet transform.[13] Rather than using prescribed frequency bands, the VMD method adaptively decomposes a signal into an ensemble of band-limited Intrinsic Mode Functions (IMF), each with its own center frequency. Herein we applied VMD to the synthetic data and obtained IMF-1, IMF-2, and IMF-3 which represents low, medium, and the high-frequency band as shown in Fig. 4.

3. Results

3.1. Acoustic wave receiving from the control group

Fig. 5 shows the time domain signals received from the control group. It can be seen that the amplitudes vary with the material types

Table 1
Waterjet operating parameters.

Target material	Waterjet pressure (MPa)	Flow rate (mL/s)	Waterjet velocity (m/s)	Standoff distance (mm)	Nozzle diameter (mm)
Shale, Sandstone, AISI 1045 Steel	High: 210–230 Low: 50–60	60	High: 593–620 Low: 289–317	2.0	0.76

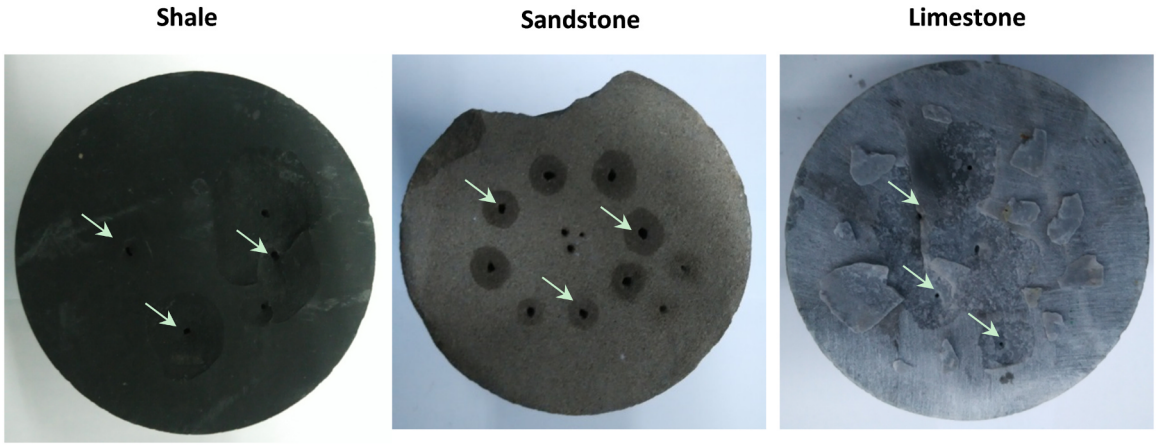

Fig. 2. Photograph of the rock drilling samples and their drilling holes.

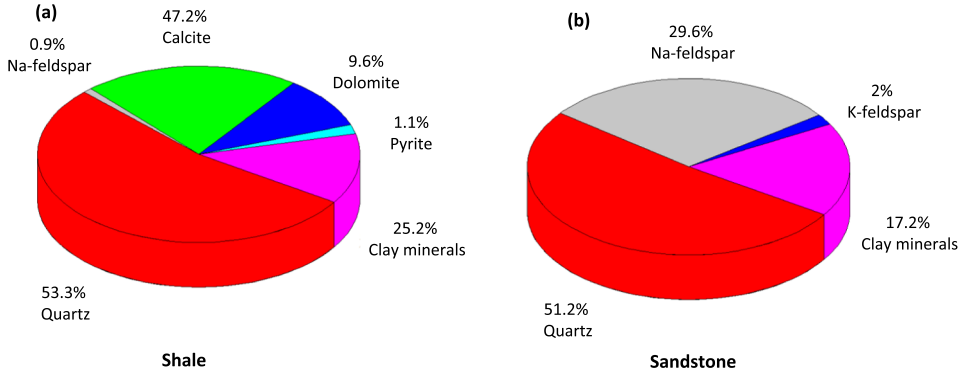

Fig. 3. Mineralogical composition of the rock specimens.

Table 2
Material properties of specimen summary.

Material name	Density (g/cm^3)	Young modulus (GPa)	Poisson's ratio (-)	Yield Strength (MPa)	Shear Strength (MPa)	Longitudinal wave velocity (km/s)
Shale	2.58	28.1	0.14	228.1	72.8	3.30
Sandstone	2.24	9.8	0.24	110.7	25.5	2.09
Limestone	2.86	51.1	0.23	216.1	46.9	4.23
AISI 1045 Steel	7.89	200	0.29	275.0	/	5.90

Table 3
Experimental schemes for the control group and experimental group, respectively.

Group name	Waterjet pressure MPa	Standoff distance Mm	Treatment time min	Target material	Material failure
Control Group	50–60	2.0	1	AISI 1045	No
			1	Shale	No
			1	Sandstone	No
			1	Limestone	No
Experimental group	210–230	2.0	1	AISI 1045	No
			1–8	Shale	Yes
			1–8	Sandstone	Yes
			1–8	Limestone	Yes

and frequency band. For example, the AISI 1045 steel and shale exhibits bigger amplitude than the sandstone and limestone. Because there is no material failure within the control group, it can be inferred that the acoustic wave only from the waterjet impact is controlled by the material types.

The frequency domain was obtained from time domain signals by using the Fourier transform. First, the frequency domains of all four materials were compared as shown in Fig. 6. Although the control group excluded the material failure, yet their frequency distributions of AISI 1045 steel and the other three types of rock were still not the same even for the same waterjet impact parameters. It can be inferred that the acoustic wave is probably influenced by the material properties, particularly the acoustic characteristic of the target material. One of the potential material properties is the acoustic attenuation that measures

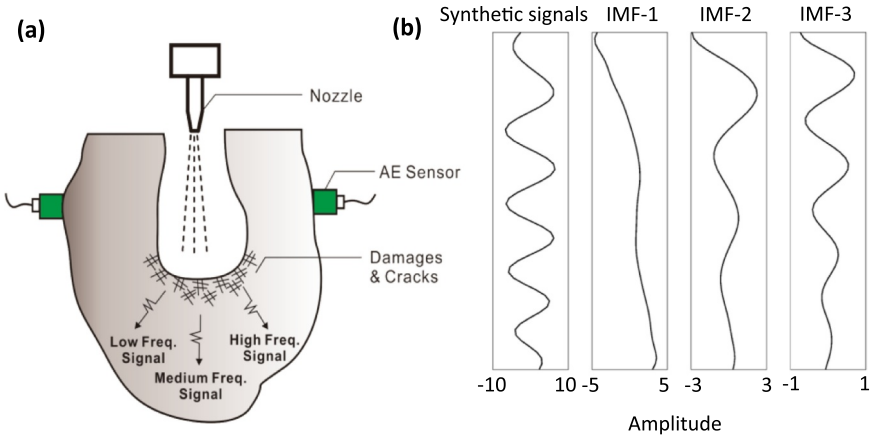

Fig. 4. (a) Schematic of synthetic signals were decomposed into three frequency bands, e.g. low, medium, and high-frequency components. (b) Schematic of Variational Mode Decomposition method.

the energy dissipation of sound propagation in media[18]. The acoustic attenuation for various rock types has been evaluated. Among those target materials studied in this study, the biggest value of acoustic attenuation is sandstone, followed by limestone, shale and AISI 1045 steel. The big value of acoustic attenuation denotes a large energy dissipation while acoustic wave propagation. It can be explained that the amplitude and frequency band of AISI 1045 and shale are bigger and wider than that of sandstone and limestone. The amplitude of medium and high-frequency components of sandstone and limestone was much weak comparing with their low-frequency components.

Moreover, the frequency domains of the control and experimental groups of AISI 1045 were compared as shown in Fig. 7. The results reconfirmed the waterjet impact was capable to generate an acoustic wave. Furthermore, a wide frequency band from 50 kHz to 500 kHz was acquired for either low waterjet pressure impact or high waterjet pressure impact. Three obviously main frequencies at 100, 250, and 400 kHz are stable. The probable mechanisms can be summarized as the waterjet impact force induces the sample vibration and then the acoustic wave is created and transmits through the sample, which is ultimately received by the AE sensor. Furthermore, it was noticed that the waterjet pressure did not affect the frequency band distribution, but influenced the amplitude of AE signals.

3.2. Signal comparison between the control and experimental groups

Fig. 8 shows the time domain signals of rock failure cases and no failure cases. The amplitude of rock failure cases is obviously bigger than that of no failure cases. The reason is that high waterjet pressure

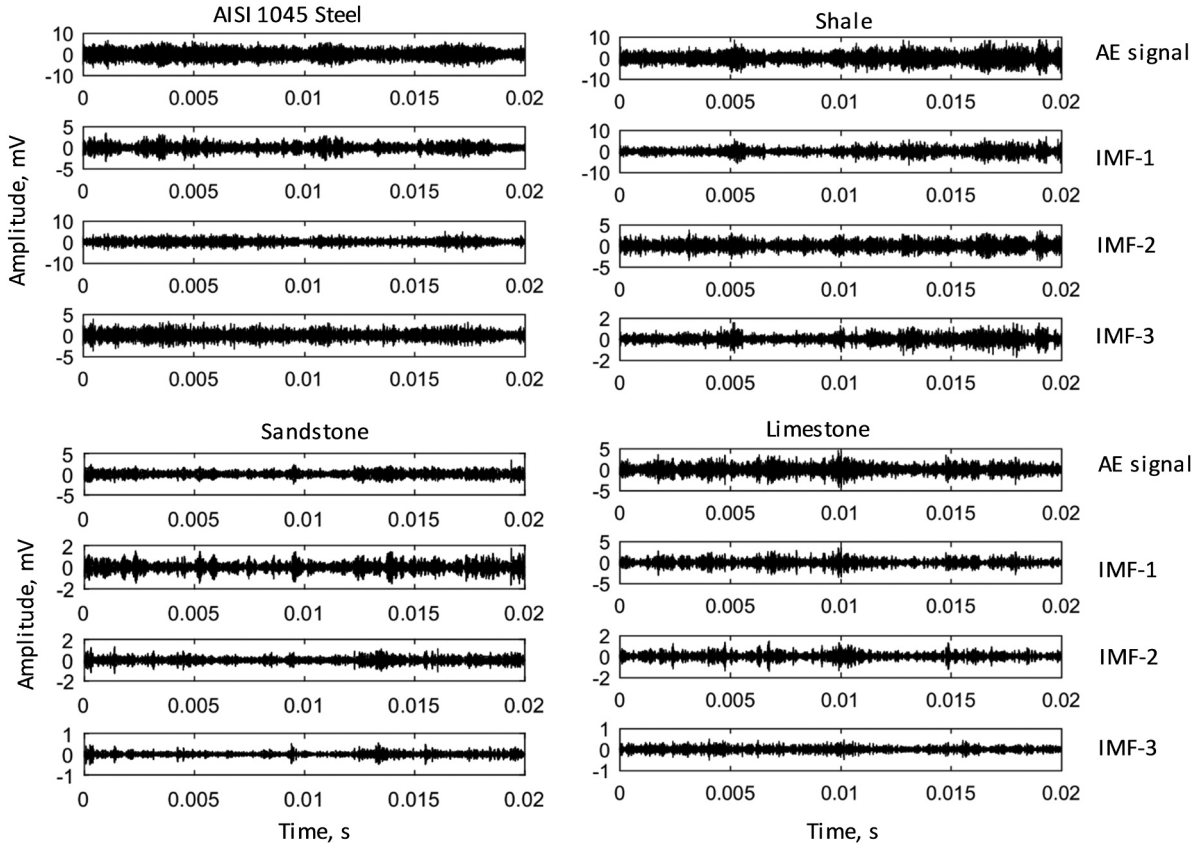

Fig. 5. The time domain signals for different materials and the synthetic signals were decomposed into three IMFs.

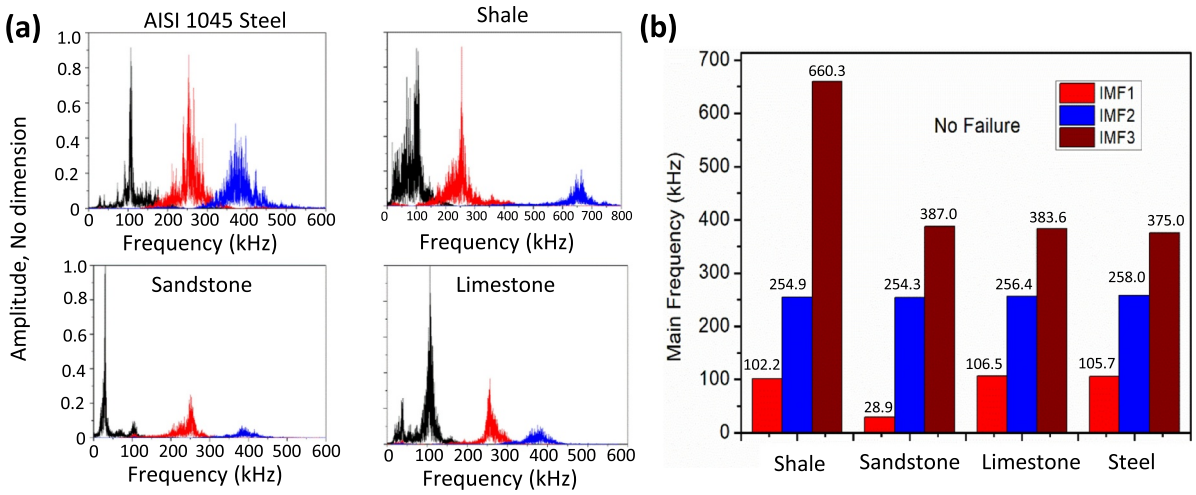

Fig. 6. (a) Frequency domain, Waterjet pressure is set as 50–60 MPa below the yield strength of those rock samples. The macro failure does not occur during waterjet impact. (b) Comparison of the main frequency for the corresponding frequency signals.

provides more energy input. Furthermore, the energy release from material failure also provides extra energy for the acoustic wave. Particularly, the amplitude of shale rock failure has the biggest value as compared with the other two rocks, since the energy dissipation of acoustic wave propagating in shale medium is relatively small.

The frequency domain between the control and experimental groups were compared as shown in Fig. 9. It is obvious that the frequency band becomes narrow while rock failure occurs. The only difference between the control and experimental groups is whether the rock failure or not. Thus, the results demonstrated that rock failure is the primary reason for the strong dissipation of the high-frequency signal.

The main frequency values at every minute were extracted and plotted versus drilling time as shown in Fig. 10. The main frequencies are no longer a constant but to be fluctuant. Among those three IMF components, the main frequency of the high-frequency component (IMF-3) strongly changes. However, the main frequency of medium frequency component (IMF-2) is almost a constant (254 kHz and 100 kHz for no failure and rock failure cases, respectively) whenever rock failure occurs. The results reconfirmed the high-frequency signals are the indicator of rock failure behaviors. It is well known that the high-frequency signals belong to shortwave signal and are easily dissipated that results in propagation of the microcracks. Recent studies also indicated that the dissipation of the high-frequency signals is positively related to the density of crack generation.[15,16] Therefore, the frequency reduction of the high-frequency signals is able to be an indicator to reflect the rock cracking intensity.

We correlated the main frequency of three frequency band with the rate of penetration as shown in Fig. 11. The high-frequency band presented a good correlation with the Rate of Penetration (ROP) because of the relatively high R-squared values. In details, shale performed a negative correlation with ROP; sandstone samples present a positive correlation with ROP, and Limestone samples behaved a steady main frequency of the high-frequency band. The results suggested that the crack density of the shale failure increases with the increasing of ROP. However, the crack density of the sandstone failure decreases and the limestone generated a steady crack density. The various observations may cause from their specific rock failure mechanisms.

4. Discussion

4.1. Characteristics of acoustic wave purely from waterjet impact

The control group was specially designed for investigating the characteristics of acoustic wave induced by waterjet impact. Our results clearly demonstrated that the waterjet impact generates a wideband acoustic signal. Both the amplitude and frequency domain of acoustic wave varies with the material types. Particularly, the frequency distribution of the high-frequency signals exhibited a strong diversity among those four materials in this study. The acoustic attenuation provided a good explanation of those observations. It can be explained that the higher acoustic attenuation that the material owns, the less occurrence of the high-frequency signals.

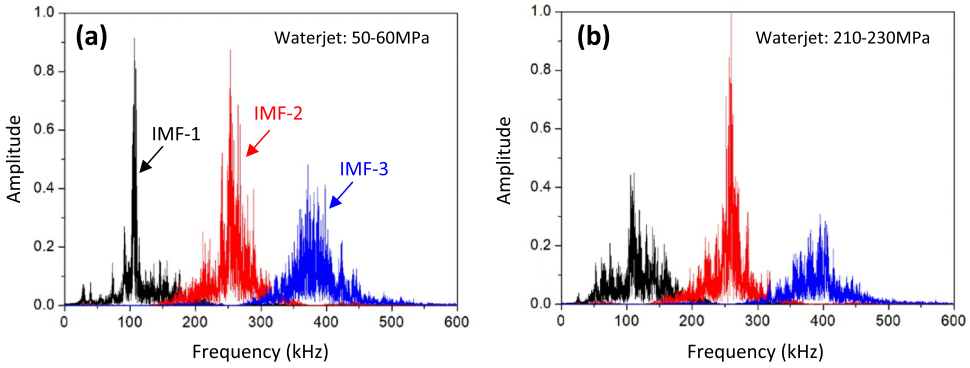

Fig. 7. Frequency domain of acoustic signals of AISI 1045 steel under waterjet impact (a) control group, (b) experimental group. Waterjet pressure is controlled below the yield stress of AISI 1045 steel.

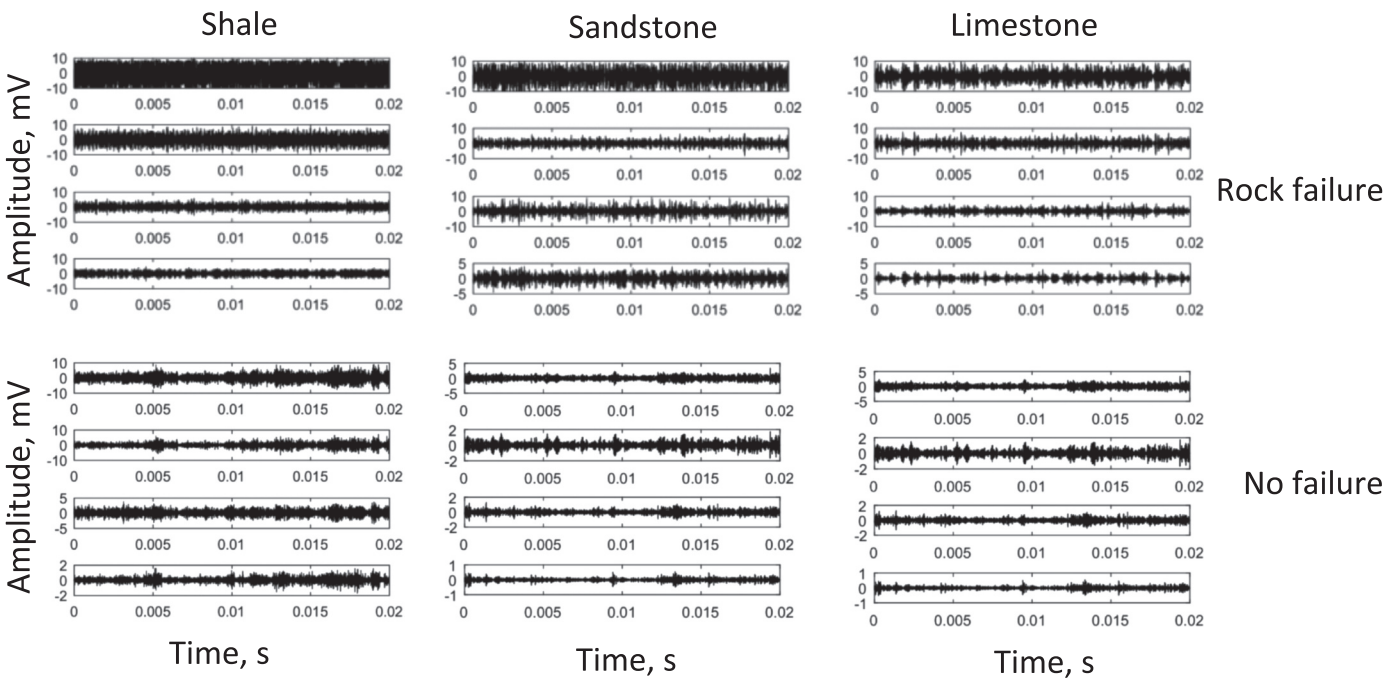

Fig. 8. AE Time domain signals of rock materials while waterjet drilling process. The amplitude of rock failure cases is much bigger than that of no failure cases.

In this study, we also found the main frequency of the medium-frequency signals from all four materials was kept at the same value. A reasonable explanation is that the frequency band represents the characteristics of waterjet but not the material properties. If the waterjet parameter does not change, the main frequency will not change.

Furthermore, the waterjet pressure did not change the frequency domain distribution of the material. Thus, the waterjet maybe a good seismic generator to generate acoustic signals with a considerable bandwidth. The frequency domain is capable to be used for identifying the formation lithology and wave propagation properties of rock while underground drilling.

4.2. Identification of acoustic emission from rock failure

While waterjet rock drilling, an obvious reduction of the high-frequency signals was observed and the frequency domain distribution move to the left low-frequency domain. Furthermore, the main frequency of high-frequency signals starts to be time-dependent that

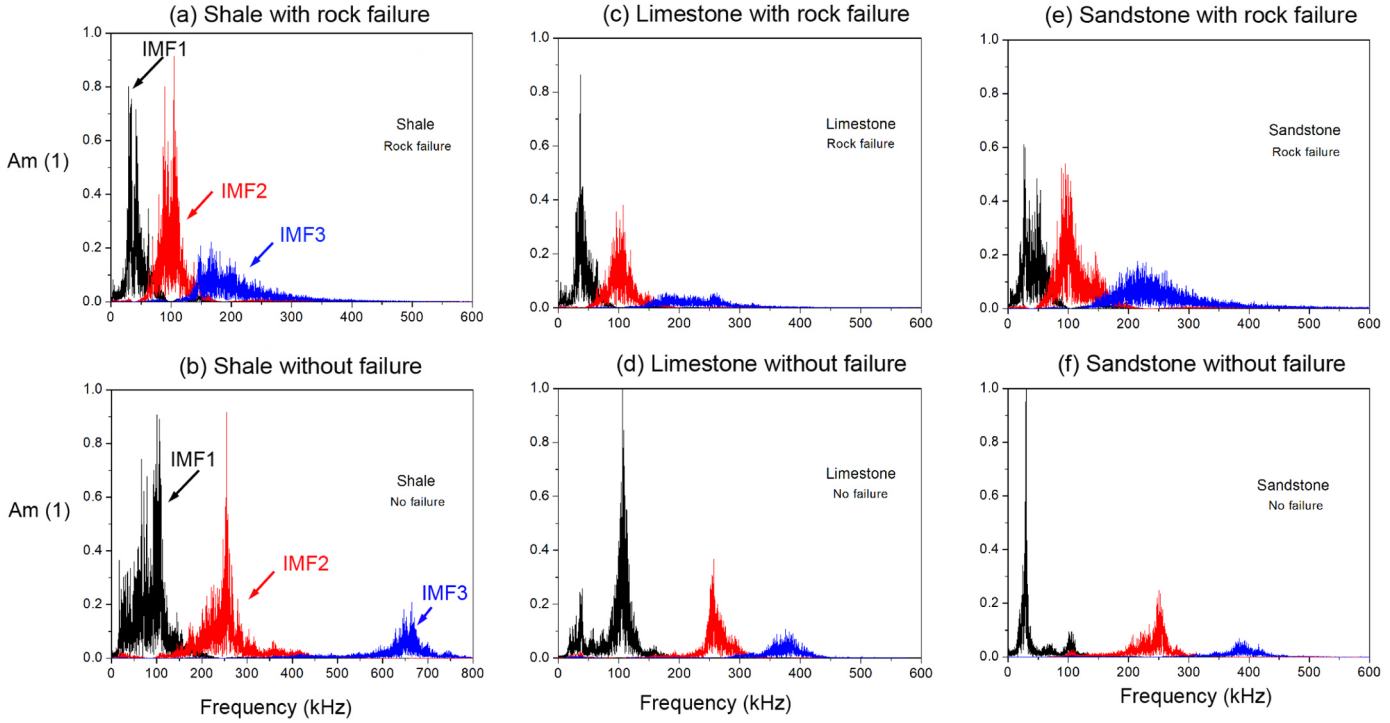

Fig. 9. AE Frequency signals of rock materials while waterjet drilling process. The amplitude and frequency distribution differed from rock lithology and IMF components.

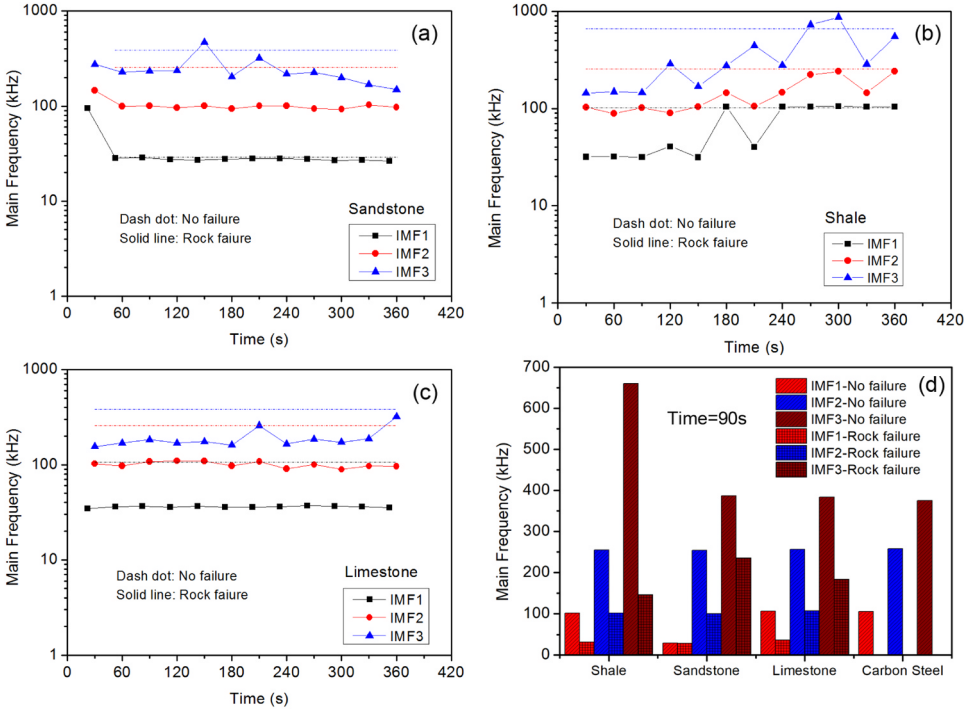

Fig. 10. Comparison of the main frequency distribution of Unique AE source and Multiple AE sources. (a) Sandstone sample, (b) Shale sample, (c) Histogram of main frequency at a specific time.

causes from the rock failure process, i.e., cracking or damaging in the mineral scale. The CT scan imaging provided the evidence of the microcracks in hundreds of micrometers in sandstone samples. Because of the occurrence of the cracks and damages, the shortwave signals were dissipated through propagating those flaws. That is why the high-frequency signals eliminate seriously from rock failure.

Fortunately, the previous studies confirmed that the AE frequency can be used to characterize the microcracking processes leading to failure.[14] Thus, it is believed that the fluctuation of the main frequency in this study actually reflected the cracking intensity. The good correlation between the main frequency of high-frequency signals and ROP also supported this explanation. It is interesting that the trend of the correlation curve probably reveals the rock failure mechanics. For example, the crack intensity of shale failure is low for a big value of ROP. Reversely, the crack intensity of sandstone failure is relatively high for a big value of ROP. The CT scan images prove this observation again, where the shale under waterjet impact tends to be crushed in the manner of mineral erosion, but the sandstone is prior to creating cracks to be volumetric break.[17] This study reconfirms the acoustic emission is capable to identify the rock failure behaviors and can be used for waterjet rock drilling monitoring.

5. Conclusions

A series of acoustic emission monitoring experiments were conducted to identify the signal sources from waterjet rock drilling process. An advanced frequency analysis, variational mode decomposition (VMD) approach, was used to decompose the synthetic signal into the low, medium, and high-frequency signals. First, the waterjet impact is capable to generate a wideband acoustic signal. The acoustic attenuation of the material strongly influences the amplitude and frequency domain distribution of acoustic wave. Furthermore, the waterjet pressure did not change the frequency domain distribution of the material. Second, an obvious reduction of the high-frequency signals was observed while waterjet rock drilling. Moreover, the main frequency of high-frequency signals starts to be time-dependent that causes from the rock failure process, i.e., cracking or damaging in the mineral scale. The good correlation between the main frequency of high-frequency signals and ROP also supported this explanation. It is interesting that the trend of the correlation curve probably reveals the rock failure mechanics.

The waterjet maybe a good seismic generator to generate acoustic signals in order to identify the formation lithology and wave propagation properties of rock while underground drilling. Besides, this study

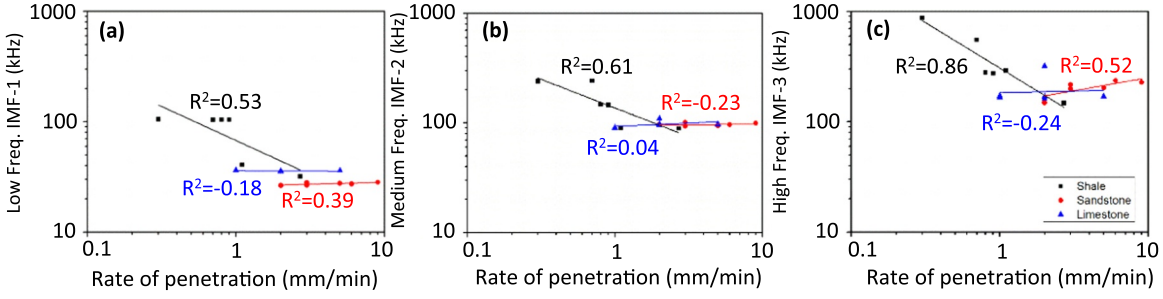

Fig. 11. Correlation of the main frequency of three frequency bands and ROP. (a) Low-frequency band; (b) Medium frequency band; (c) High-frequency band.

reconfirms the acoustic emission is capable to identify the rock failure behaviors and can be used for waterjet rock drilling monitoring.

Acknowledgments

This work was financially supported by the National Natural Science Foundation of China (Nos. 51704308, U1562212 & 51490652) and Science Foundation of China University of Petroleum, Beijing (No. 2462014YJRC048). Authors many thank reviewers for their valuable comments to improve our quality. Authors also thank Dr. Xiaoqiong Wang and Dr. Shan Wu for their valuable discussion.

References

1. Lindley T, Palmer I, Richards C. Acoustic emission monitoring of fatigue crack growth. *Mater Sci Eng.* 1978;32:1–15.
2. Conway GJ. Acoustic emission monitoring. *J Acoust Soc Am.* 1986;79 [589-589].
3. Brook N, Summers DA. The penetration of rock by high-speed water jets. *Int J Rock Mech Min Sci.* 1969;6:249–258.
4. Kovacevic R, Kwak H, Mohan R. Acoustic emission sensing as a tool for understanding the mechanisms of abrasive water jet drilling of difficult-to-machine materials. *Proc Inst Mech Eng Part B: J Eng Manuf.* 1998;212:45–58.
5. Tian S, Sheng M, Li Z, Ge H, Li G. Acoustic emission characteristics of sedimentary rocks under high-velocity waterjet impingement. *Rock Mech Rock Eng.* 2017;50:2785–2794.
6. Mohan R, Momber A, Kovacevic R. On-line monitoring of depth of AWJ penetration using acoustic emission technique. *Jet Cutting Technology*. London: Mechanical Engineering Publications; 1994:649–664.
7. Momber A, Mohan R, Kovacevic R. On-line analysis of hydro-abrasive erosion of pre-cracked materials by acoustic emission. *Theor Appl Fract Mech.* 1999;31:1–17.
8. Momber AW. Energy transfer during the mixing of air and solid particles into a high-speed waterjet: an impact-force study. *Exp Therm Fluid Sci.* 2001;25:31–41.
9. Mohan R, Momber A, Kovacevic R. Energy dissipation control in hydro-abrasive machining using quantitative acoustic emission. *Int J Adv Manuf Technol.* 2002;20:397–406.
10. Hassan AI, Chen C, Kovacevic R. On-line monitoring of depth of cut in AWJ cutting. *Int J Mach Tools Manuf.* 2004;44:595–605.
11. Axinte D, Kong M. An integrated monitoring method to supervise waterjet machining. *CIRP Ann Manuf Technol.* 2009;58:303–306.
12. Rabani A, Marinescu I, Axinte D. Acoustic emission energy transfer rate: a method for monitoring abrasive waterjet milling. *Int J Mach Tools Manuf.* 2012;61:80–89.
13. Li F, Zhang B, Zhai R, Zhou H, Marfurt KJ. Depositional sequence characterization based on seismic variational mode decomposition. *Interpretation.* 2017;5:SE97–SE106.
14. Ohnaka M, Mogi K. Frequency characteristics of acoustic emission in rocks under uniaxial compression and its relation to the fracturing process to failure. *J Geophys Res Solid Earth.* 1982;87:3873–3884.
15. Crampin S, McGonigle R, Bamford D. Estimating crack parameters from observations of P-wave velocity anisotropy. *Geophysics.* 1980;45:345–360.
16. Hall SA, Kendall JM, Maddock J, Fisher Q. Crack density tensor inversion for analysis of changes in rock frame architecture. *Geophys J Int.* 2008;173:577–592.
17. Sheng M, Tian S, Li G, Ge H, Li Z, Cheng Z. Experimental study on rock failure of organic-rich shale caused by waterjet impinging, In: *Proc. of 51st U.S. Rock Mechanics/Geomechanics Symposium*, San Francisco; 2017.
18. Jongmans D. In-situ attenuation measurements in soils. *Eng Geol.* 1990;29:99–118.